Design and Simulation Analysis of a Parabolic Trough Solar Collector Hot Water Generation System

A. Valan Arasu and T. Sornakumar

Department of Mechanical Engineering
Thiagarajar College of Engineering
Madurai – 625 015
Tamilnadu
INDIA

www.serd.ait.ac.th/reric

ABSTRACT

Collection of solar energy with the help of a cylindrical parabolic concentrator has been the subject of many investigations. A parabolic trough collector (PTC) system used for hot water generation is presented in this paper. The design of a parabolic trough collector with 90º rim angle is accomplished by considering the optimized collector aperture width and the receiver tube diameter. The simulation program written in MATLAB is used to predict the performance of the parabolic trough collector hot water generation system. The effects of variations in water inlet temperature, mass flow rate, annulus gap and wind velocity on optical and thermal performance of the collector have been analysed.

1.   INTRODUCTION

The two main approaches, namely, thermal devices and photovoltaic devices popularly known as solar cells, are being followed to utilize solar energy. Current applications for the conversion of solar radiation to thermal energy are being directed towards the achievement of elevated temperatures. To achieve this objective, the parabolic trough collector (PTC) is currently receiving considerable attention, despite the fact that this solar concentrating device requires some level of solar tracking. The disadvantage inherent with this tracking requirement is apparently offset by the advantage associated with the high order of concentration available with this collector. The most suitable mode of one axis tracking is east-west horizontal mode as its performance is very close to full or two axis tracking [1]. This tracking mode has very small shadowing effects especially in multi-collector installations and is very less sensitive to misalignment. Hence, the mode of tracking employed in the present work is the east-west horizontal i.e. the parabolic trough collector axis is oriented in a north-south direction and the collector tracks the sun in an east-west direction. The design of the collector must be such that energy collection is high, thermal losses are low and the effectiveness to cost ratio is as high as possible. Heinzel et al [2] have developed an optical model of a parabolic trough collector and used with a basic heat loss model to simulate the Luz System Two (LS2) trough collector, used in the Solar Thermal Electric Generation (SEGS) plant at Kramer Junction in Southern California, which uses synthetic oil as the working fluid. The model shows good agreement with the test results reported by Dudley et al [3]. Odeh et al [4, 5] have developed a model of thermal losses from the measurement of thermal performance of parabolic trough solar collector using Syltherm 800 oil as the working fluid at Sandia National Laboratory. In the present work, a detailed analysis of the thermal performance of a 90º rim angle parabolic trough collector for hot water generation is carried out. A simulation model based on the MATLAB software has been developed to optimise the collector important geometry and to study the effect of some important parameters on the performance of the collector.

2.   DESIGN OF PARABOLIC TROUGH COLLECTOR

2.1   Performance Parameters of PTC

One measure of the performance of a PTC is the optical efficiency (η_o), defined as the ratio of the energy absorbed by the receiver to the energy incident on the concentrator's aperture [6]. The optical efficiency value depends on the optical properties of the materials involved, the geometry of the collector, and the various imperfections arising from the construction of the collector. It is expressed as [1],

$$\eta_o = \rho_m \tau_e \alpha_r \gamma \left[\left(1 - A_f \tan \theta \right) \cos \theta \right] \tag{1}$$

where ρ_m is the mirror or reflector reflectance, τ_e is the transmittance of envelop material, α_r is the receiver absorptivity, γ is the intercept factor, A_f is the geometric factor and θ is the angle of incidence.

The intercept factor, γ is defined as the ratio of the energy intercepted by the receiver to the energy reflected by the focusing device [6]. The value of intercept factor depends on the size of the receiver, the surface angle errors of the parabolic mirror and solar beam spread. According to Guven and Bannerot [7], these errors or imperfections are of two types, namely random and non-random.

Random errors are defined as those errors, which are truly random in nature and therefore can be represented by normal probability distributions. These errors are identified as apparent changes of the sun's width, scattering effects caused by random slope-errors (i.e. distortion of the parabola due to wind loading) and scattering effects associated with the reflective surface. Random errors are modeled statistically, by total reflected-energy distribution standard deviations σ at normal incidence,

$$\sigma = \sqrt{\sigma_{sun}^2 + 4\sigma_{slope}^2 + \sigma_{mirror}^2}$$

where, σ_{sun} = Standard deviation of the energy distribution of the sun's rays at normal incidence.
σ_{slope} = Standard deviation of the distribution of local slope errors at normal incidence.
σ_{mirror} = Standard deviation of the variation in diffusivity of the reflective material at normal incidence.

Non random errors are determined by the misalignment angle error β (i.e. the angle between the reflected ray from the center of the Sun and the normal to the reflector's aperture plane) and the displacement of the receiver from the focus of the parabola dr.

According to Guven and Bannerot [8], random and non-random errors can be combined with the collector's geometric parameters, concentration ratio, C and receiver tube diameter, $D_{r,o}$ to yield error parameters universal to all collector geometries. These are called 'Universal Error Parameters'. These parameters are distinguished from already defined parameters by a superscript asterisk* and are defined as,

Universal random error parameter $\sigma^* = \sigma C$
Universal nonrandom error parameter due to angular errors $\beta^* = \beta C$ and
Universal nonrandom error parameter due to receiver dislocation and reflector profile errors $d^* = dr/D_{r,o}$

For the evaluation of the intercept factor   a closed-form expression developed by Guven and Bannerot [7] is used,

$$\gamma = \frac{1 + \cos \phi_r}{2 \sin \phi_r} \int_0^{\phi_r} Erf\left(\frac{\sin \phi_r (1 + \cos \phi)(1 - 2d^* \sin \phi) - (\pi\beta^*(1 + \cos \phi_r))}{\sqrt{2}\pi\sigma^*(1 + \cos \phi_r)} \right) -$$
$$Erf\left(-\frac{\sin \phi_r (1 + \cos \phi)(1 + 2d^* \sin \phi) + (\pi\beta^*(1 + \cos \phi_r))}{\sqrt{2}\pi\sigma^*(1 + \cos \phi_r)} \right) \frac{d\phi}{(1 + \cos \phi)} \tag{2}$$

where ϕ_r is collector rim angle, defined as the angle subtended by the edges of the reflector at the focus.

A simple MATLAB program, which numerically evaluates the above expression, is developed. The intercept factor program flow chart is shown in figure 1. The principle of operation of the program is that the two error functions are computed and then the integral is numerically integrated using Simpson integration method for one degree steps of angle ϕ for ϕ between 1° and $\phi_r = 90$ °. The calculated values are added up and finally divided by the number of steps to get the intercept factor value.

Start

Input Data σ^*, β^*, d^* and $\phi_r = 90^o$

$\phi = 0$ to ϕ_r step 1^O

Evaluate Two Error Functions

Calculate Intercept Factor Using Simpson Integration Method

Add Calculated Value to the Previous Value

Next ϕ

Intercept Factor (γ) = Total Value / Number of Steps
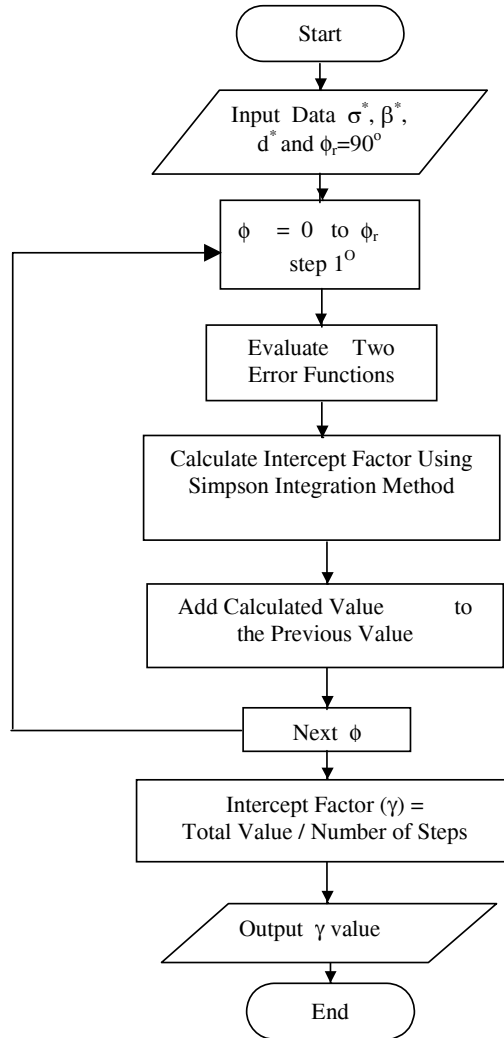
Output γ value

End

Fig.1. Intercept factor program flow chart.

The geometric factor A_f is a measure of the effective reduction of the aperture area due to abnormal incidence effects [1] and it is given by,

$$A_f = \frac{\frac{2}{3} W_a h_p + f W_a \left(1 + \frac{W_a^2}{48 f^2} \right)}{A_a} \qquad (3)$$

where W_a is the aperture width (m), h_p is the parabola height (m), f is the focal distance (m), and A_a is the collector aperture area (m²). The parabolic trough collector dimensions are shown in figure 2.
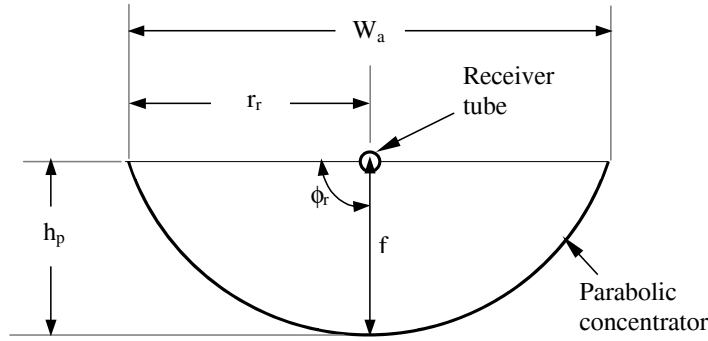
Fig. 2. Parabolic trough collector dimensions.

Another important performance parameter is the thermal efficiency (η), defined as the rate at which useful energy (Q_u) is delivered to the working fluid per unit of aperture area divided by the beam solar flux (I) at the collector's aperture plane. The thermal efficiency h may be calculated from an energy balance on the receiver [6,9], which is given by,

$$\eta = \frac{Q_u}{IA_a} = \frac{\eta_o IA_a - U_L(T_r - T_a)A_r}{IA_a} = \eta_o - \left(\frac{U_L(T_r - T_a)}{I \times C}\right) = \frac{\dot{m}c_p(T_{fo} - T_{fi})}{IA_a} \tag{4}$$

where U_L is the overall heat loss co-efficient (W/m²K), T_r is the mean receiver surface temperature (K), T_a is the ambient air temperature (K), I is direct solar radiation (W/m²), A_r is the receiver tube area, $\dot{m}$ is mass flow rate (kg/s), T_{fi} is water inlet temperature (K), T_{fo} is water outlet temperature (K) and c_p is specific heat capacity of water (J/kg-K).

The overall heat loss co-efficient from the absorber tube surface to the surroundings is given by,

$$U_L = \frac{Q_l}{\Pi D_{r,o}L(T_r - T_a)} \tag{5}$$

where L is receiver tube length (m).

The overall heat loss (Q_l) from the collector is established by applying heat balance on the receiver tube [6,10],

$$Q_l = Q_{r-e} \tag{6}$$

where Q_{r-e} is heat loss by radiation $Q_{r(r-e)}$ and convection $Q_{c(r-e)}$ due to stationary air between the receiver tube and the glass envelope i.e.,

$$Q_{r-e} = Q_{r(r-e)} + Q_{c(r-e)} \tag{7}$$

The radiation heat transfer between the absorber tube and the glass envelope is given by [11],

$$Q_{r(r-e)} = \frac{\sigma\left(T_r^4 - T_e^4\right)\Pi D_{r,o}L}{\left[\frac{1}{\varepsilon_r} + \frac{1 - \varepsilon_e}{\varepsilon_e}\left(\frac{D_{r,o}}{D_{e,i}}\right)\right]} \tag{8}$$

where σ is Stefan-Boltzmann constant, (= 5.670 x 10⁻⁸ W/m² - K⁴), T_e is the glass envelope surface temperature (K), ε_r is the emissivity of receiver tube surface (0.1 assumed), ε_e is the emissivity of glass envelope (0.9 assumed) and $D_{e,i}$ is the glass envelop inner diameter (m).

The heat transfer by convection due to the motionless air in the annulus between the receiver tube and glass envelope may be expressed as [11],

$$Q_{c(r-e)} = \frac{2\Pi k_{eff}}{\ln(D_{e,i}/D_{r,o})} (T_r - T_e) \tag{9}$$

where the effective thermal conductivity k_{eff} is the thermal conductivity that a stationary fluid should have to transfer the same amount of heat as the moving fluid.

The correlation for k_{eff} is,

$$\frac{k_{eff}}{k} = 0.386 \left(\frac{Pr}{0.861 + Pr} \right)^{0.25} (Ra_c^*)^{0.25}$$

where k is the thermal conductivity of air and Pr is Prandtl number. Ra_c^* is modified Rayleigh number and is related to the usual Rayleigh number by the following equation [11],

$$Ra_c^* = \frac{[\ln(D_{e,i}/D_{r,o})]^4}{L_g^3 (D_{r,o}^{-0.6} + D_{e,i}^{-0.6})^5} Ra_L$$

and

$$Ra_L = \frac{g\beta(T_r - T_e)L_g^3}{v\alpha}$$

where annulus gap, $Lg = (D_{e,i} - D_{r,o})/2$, v is the kinematic viscosity of air, a is thermal diffusivity of air and $\beta = \frac{1}{T_m}$. The mean temperature of air at which the properties of air are evaluated is,

$$T_m = \frac{T_r + T_e}{2}$$

The convective heat transfer coefficient h_w on the inside surface of the receiver tube can be calculated under the assumption that the flow is fully developed,

$$h_w = Nu_D \left(\frac{k_w}{D_{r,i}} \right) \tag{10}$$

where k_w is the thermal conductivity of water and $D_{r,i}$ is the receiver tube inner diameter.

The Nusselt number for a laminar, fully developed flow conditions with a constant surface heat flux is given by [11],

$$Nu_D = 4.36$$

For a turbulent flow (Reynolds Number $Re_D > 2000$), the Nusselt number may be calculated from the well known Dittus-Boelter equation [11],

$$Nu_D = 0.023 \, Re_D^{0.8} \, pr^{0.4}$$

where $Re_D = \frac{V_f D_{r,i}}{v_f}$, V_f is the velocity of water and v_f is the kinematic viscosity of water. All properties of water are evaluated at the bulk mean temperature,

$$T_b = \frac{T_{fo} + T_{fi}}{2}$$

The concentration ratio is defined as the ratio of aperture area (A_a) to receiver area (A_r).

$$C = \frac{A_a}{A_r} = \frac{W_a L}{\Pi D_{r,o} L} \tag{11}$$

The parabola aperture width,

$$W_a = 2\, r_r \sin(\phi_r) = 4\, f \tan\left(\frac{\phi_r}{2}\right) \tag{12}$$

where r_r is the rim radius (m) and ϕ_r is the rim angle (degree).

The pressure drop needed to sustain an internal flow determines pump power requirements. It is expressed as [11],

$$\Delta P = f\, \frac{\rho_f V_f^2 L}{2 D_{r,i}} \tag{13}$$

where f is Moody or Darcy friction factor and ρ_f is the density of water.

For fully developed laminar flow,

$$f = \frac{64}{\mathrm{Re}_D}$$

and for fully developed turbulent flow ($3000 \leq \mathrm{Re}_D \leq 5 \times 10^6$),

$$f = \left(0.790 \ln(\mathrm{Re}_D) - 1.64\right)^{-2}$$

2.2   Optimisation of Collector Aperture Width

In the present work, optimization of collector aperture width and selection of receiver diameter are made using the MATLAB program developed for the evaluation of intercept factor. While the geometric factor increases, the intercept factor decreases as the aperture width increases. This variation of intercept factor with aperture width is illustrated in figure 3. The smaller the collector aperture, the smaller will be the geometric factor and higher will be the intercept factor, leading to higher optical efficiency. But, for a given receiver diameter, the concentration ratio is reduced as the aperture decreases, resulting in higher thermal losses.
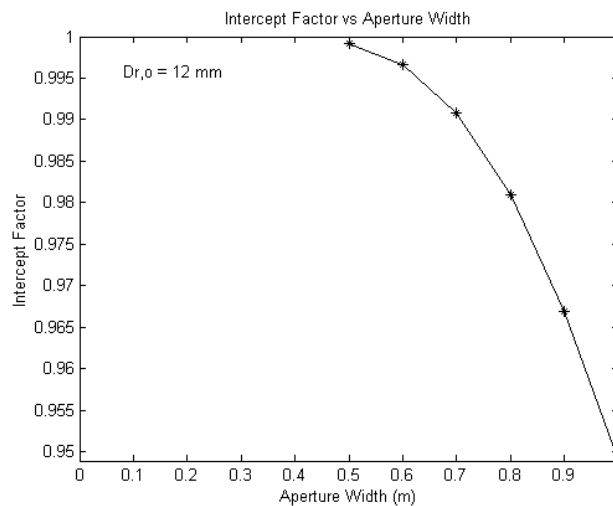

Fig. 3. Variation of intercept factor, γ with collector aperture width, W_a.

The optical efficiency is calculated using equation (1) for the solstices June 21 and December 22 at which the incidence angle is maximum and hence the geometrical effect is maximum [12]. The corresponding thermal efficiency is calculated using equation (4) and the results are plotted in Figure 4. The optical efficiency decreases continuously where as the thermal efficiency first increases with the aperture width and then decreases as shown in figure 4. This is due to the fact that the thermal losses depend on the heat loss co-efficient and receiver tube surface and ambient temperatures. Thus optimum aperture width value is selected corresponding to the maximum thermal efficiency value. In this case, the maximum thermal efficiency is for 0.8 m aperture width.
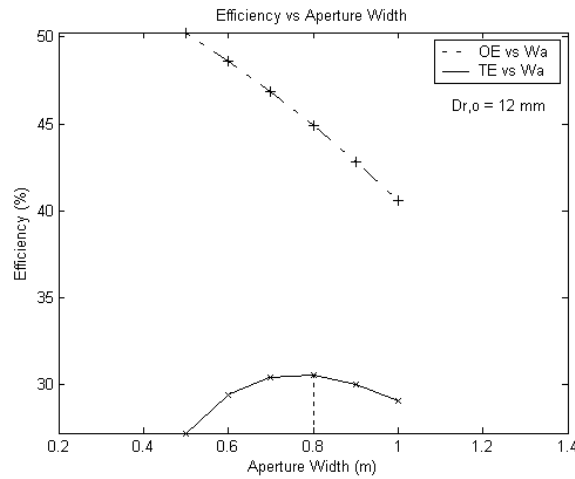

Fig. 4. Variation of optical efficiency, OE (η_o) and thermal efficiency, TE (η) with collector aperture width, (W_a).

[L = 1.25 m; ρ_m = 0.85; α_r = 0.9; τ_e = 0.9; I = 500 W/m²; U_L = 7 W/m²K; T_r = 250 ºC; T_a = 32 º]

2.3   Selection of Receiver Tube Diameter

The receiver tube diameter determines the intercept factor and consequently the optical efficiency. As the receiver tube diameter increases the value of intercept factor increases (figure 5). This effect is due to the fact that the energy intercepted by the receiver tube increases as its diameter increases, resulting in an increase in intercept factor.
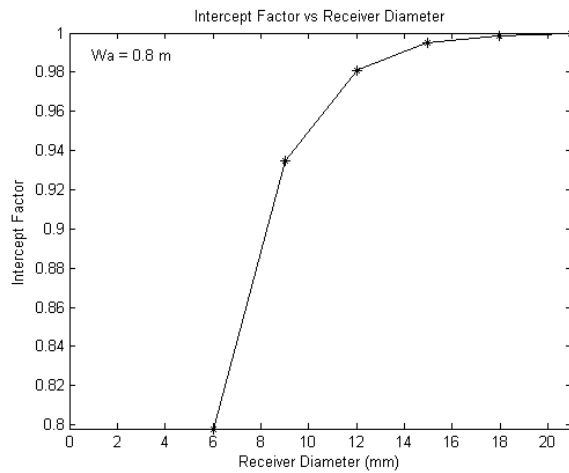

Fig. 5. Variation of intercept factor, γ with receiver tube diameter, $D_{r,o}$.

Since optical efficiency is directly proportional to intercept factor, the aim is towards a high intercept factor. Thus, higher the receiver diameter, greater will be the optical efficiency. From figure 5, the selection of the receiver diameter could be either 12 or 15 mm. But, the final selection would be based on the thermal analysis [12]. This is because the larger diameter gives a higher intercept factor but at the same time higher thermal losses. The optical and thermal efficiencies are calculated using equations (1) and (4) respectively for various diameter values from 6 mm to 21 mm and plotted in figure 6. It can be observed that the maximum thermal efficiency is for the receiver diameter of 12 mm, and is therefore selected.
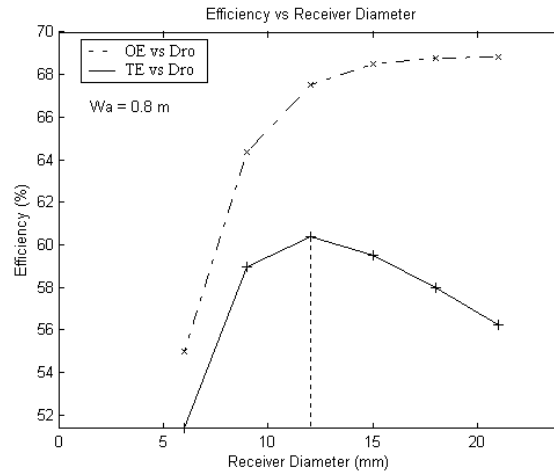

Fig. 6. Variation of optical efficiency, OE (η_o) and thermal efficiency, TE (η) with receiver tube diameter, $D_{r,o}$:
[L = 1.25 m; ρ_m = 0.85; α_r = 0.9; τ_e = 0.9; I = 1000 W/m²; U_L = 7 W/ m²K; T_r = 250 ºC; T_a = 32 ºC]

2.4   Simulation Program to Determine the Optical and Thermal Characteristics of a Parabolic Trough Collector System

In the present work, a simulation model based on MATLAB program is developed to determine the optical and thermal characteristics of a parabolic trough collector system. The program flow chart is shown in figure 7. The program gets the required input and computes the optical efficiency using equation (1) and the heat loss using equation (6) to determine the receiver tube surface temperature. The computation begins with an assumption that the receiver tube surface temperature is equal to the ambient temperature and repeated until the energy balance between the receiver and glass envelope is attained. In figure 7, Q_{lr-e} is the heat loss between the receiver tube and the glass envelope and Q_{le-a} is the heat loss between the glass envelope and the ambient. Then the overall heat loss co-efficient is computed from equation (5) and used to determine the useful heat gain and thermal efficiency from equation (4). The program has two sub programs, one for air properties and the other for water properties that are calculated at the suitable temperature as defined in the program. Applying equation (10), the convective heat transfer coefficient on the inside surface of the receiver tube is calculated. Finally, the pressure drop needed to sustain an internal flow so as to determine pump power requirement is computed using equation (13). The optical and thermal efficiencies are determined for a PTC system with aperture width 0.8 m, length 1.25 m, receiver tube diameter 12 mm and rim angle 90º for varying water inlet temperature, water flow rate, wind velocity and annulus gap between the receiver tube and glass envelope.
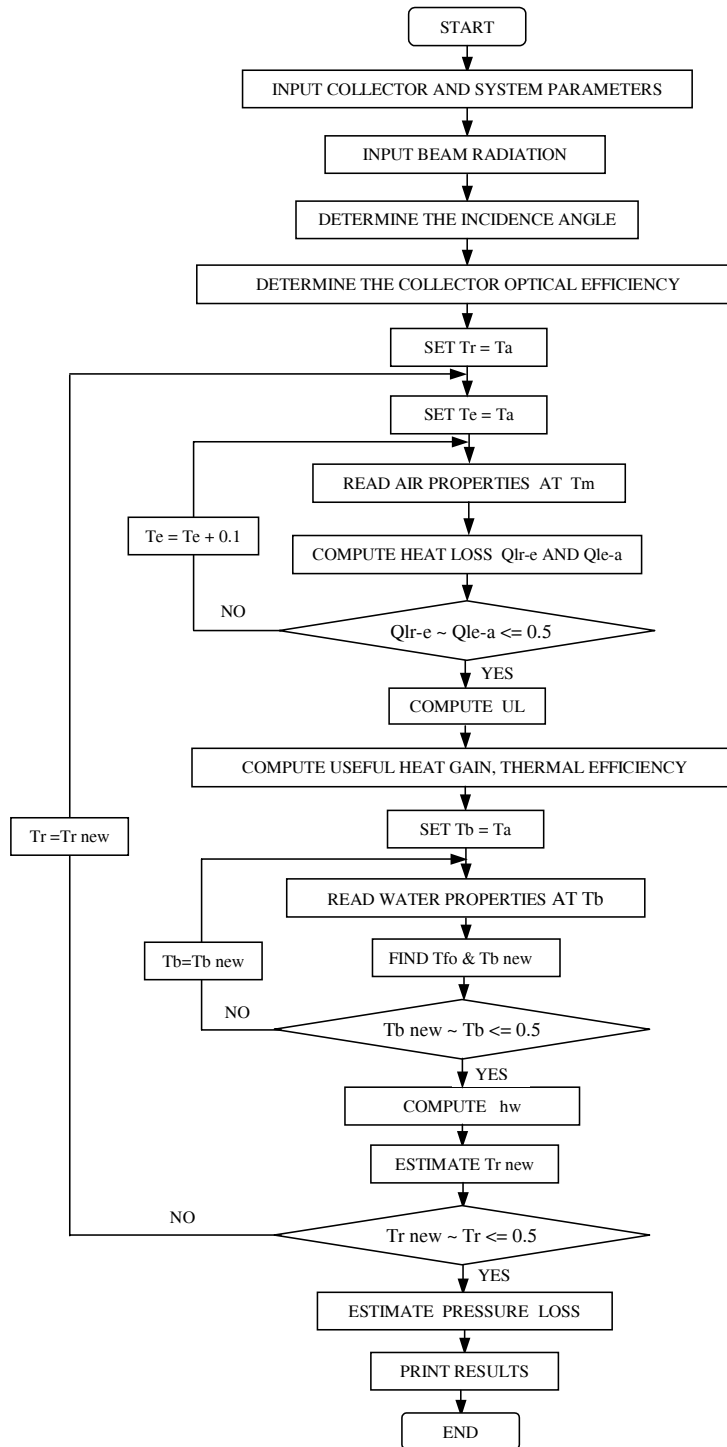
```
                          START

          INPUT COLLECTOR AND SYSTEM PARAMETERS

                  INPUT BEAM RADIATION

              DETERMINE THE INCIDENCE ANGLE

          DETERMINE THE COLLECTOR OPTICAL EFFICIENCY

                      SET Tr = Ta

                      SET Te = Ta

                  READ AIR PROPERTIES  AT  Tm

  Te = Te + 0.1     COMPUTE HEAT LOSS  Qlr-e AND Qle-a

            NO      Qlr-e ~ Qle-a <= 0.5
                            YES

                      COMPUTE  UL

          COMPUTE USEFUL HEAT GAIN, THERMAL EFFICIENCY

                      SET Tb = Ta

                  READ WATER PROPERTIES AT Tb

  Tb=Tb new         FIND Tfo & Tb new

            NO      Tb new ~ Tb <= 0.5
                            YES

                      COMPUTE  hw

                  ESTIMATE Tr new

  Tr =Tr new   NO  Tr new ~ Tr <= 0.5
                            YES

                  ESTIMATE  PRESSURE  LOSS

                      PRINT RESULTS

                          END
```

Fig. 7. Simulation program flow chart.

3.   RESULTS AND DISCUSSION

3.1   Effect of Water Inlet Temperature

As the water inlet temperature increases, the receiver tube surface temperature T_r increases. As a result, losses due to re-radiation and convection to the surroundings increase and the thermal efficiency decreases. The results of the simulation program for varying inlet temperature from 320 K to 360 K are plotted in figure 8. It is seen that the optical efficiency remains constant while the thermal efficiency decreases considerably with water inlet temperature. This is due to the fact that the value of overall loss co-efficient increases slightly as water inlet temperature increases [5]. The difference between the values of the two efficiencies is a measure of the losses due to re-radiation and convection [10].
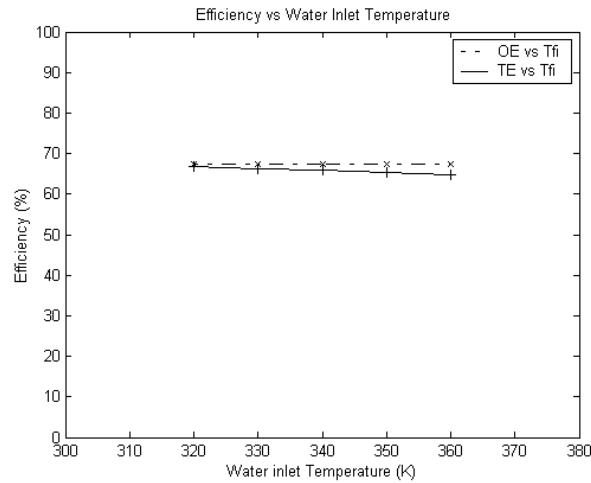

Fig. 8.   Variation of optical efficiency, OE (η_o) and thermal efficiency, TE (η) with water inlet temperature, T_{fi}

3.2   Effect of Mass Flow Rate

As the mass flow rate of water increases, the inside heat transfer co-efficient, h_w increases. As a result, the tube overall heat loss co-efficient increases and the tube surface temperature T_r decreases. Therefore, the thermal efficiency increases slightly with the increase in mass flow rate of water. At the same time the pressure drop increases, thereby increasing the demand for pumping power [4]. This effect is illustrated in figure 9 in which the mass flow rate is varied from 0.01 kg/s to 0.1 kg/s. It is seen from Figure 10 that the slope of the thermal efficiency curve keeps on decreasing with increasing values of mass flow rate until the asymptotic value is attained. Thus, an optimum value of mass flow rate could be selected as the flow rate at which the asymptotic value of thermal efficiency has almost been attained without an unduly high-pressure drop [10]. In the present case, the optimum value lies around 0.09 kg/s. It should be noted that the temperature difference $(T_{fo} - T_{fi})$ achievable depends indirectly on the mass flow rate as seen from equation (4). If the flow rate is high, the fluid has less time for heat transfer resulting in a lower temperature difference. Thus, $\dot{m}$ should be so selected that the product $\dot{m}(T_{fo} - T_{fi})$ is maximum to get the optimum thermal efficiency.
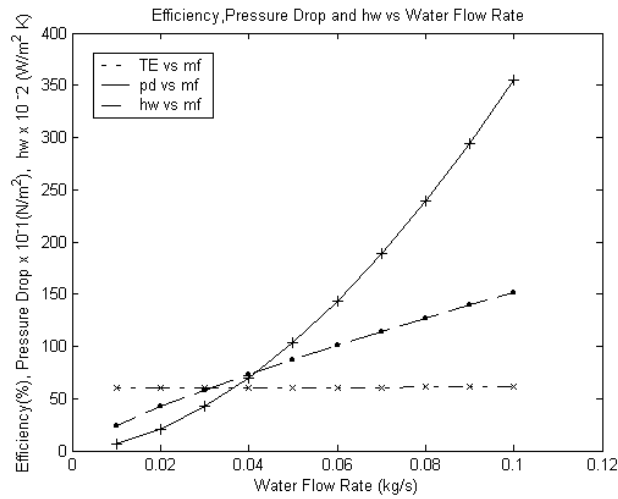
Fig. 9. Variation of thermal efficiency, TE (η), pressure drop, pd (ΔP) and convective heat transfer coefficient on the inside surface of the receiver tube, h_w with water flow rate, mf ($\dot{m}$).
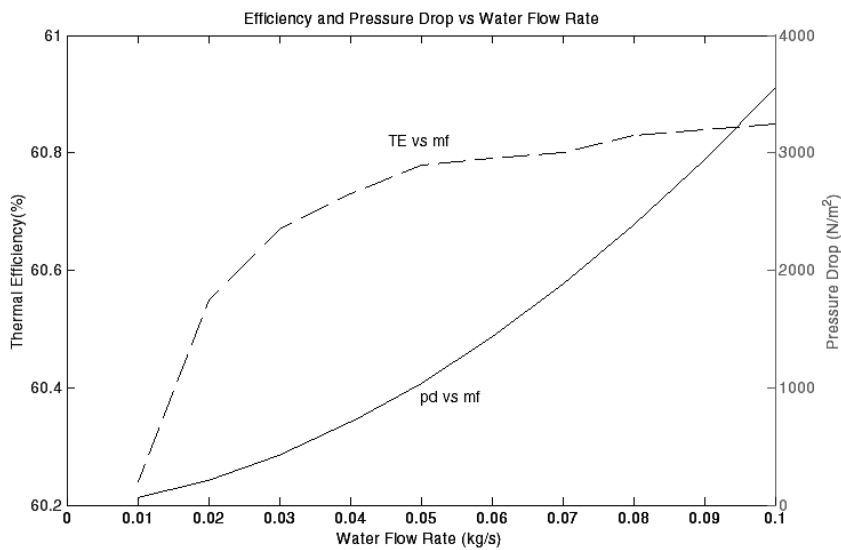

Fig. 10. Variation of thermal efficiency, TE (η) and pressure drop, pd (ΔP) with water flow rate, mf ($\dot{m}$).

3.3   Effect of Annulus Gap and Wind Velocity

Losses due to convection from the receiver tube are reduced by the use of concentric glass cover. The effect of increasing the annular space between the tube and the glass cover is shown in figure 11. It is seen that the thermal efficiency decreases with an increase in annulus gap. This is because as the annulus gap increases the tube outside convection heat transfer co-efficient increases, resulting in an increase in overall heat loss co-efficient, U_L [10].
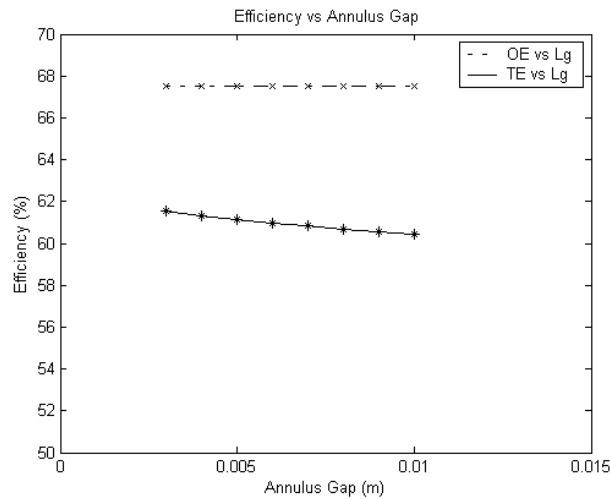
Fig.11. Variation of optical efficiency, OE (η_o) and thermal efficiency, TE (η) with annulus gap, L_g.

The effect of wind velocity on thermal efficiency is depicted in figure 12. Thermal efficiency decreases with an increase in wind velocity [4]. This is due to the increase in the glass cover outside heat transfer co-efficient and hence the overall heat loss co-efficient, U_L.
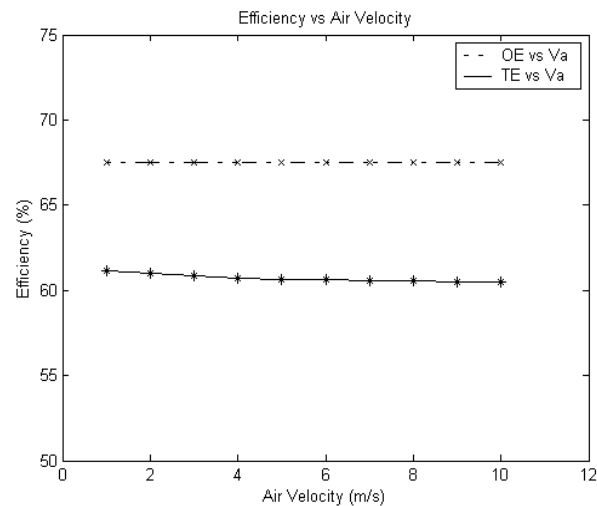

Fig. 12. Variation of optical efficiency, OE (η_o) and thermal efficiency, TE (η) with air velocity, V_a.

4.   CONCLUSION

In the present work, the modeling of a PTC system has been accomplished by performing optimization of the collector aperture width and the selection of the receiver tube diameter. The optimum values of collector aperture width and receiver tube diameter are selected corresponding to the maximum thermal efficiency value. The simulation program developed in the present work has been used to predict the effect of each of the performance parameters such as water inlet temperature and flow rate, annulus gap and wind velocity on the thermal and optical characteristics of the parabolic trough collector. The results from the simulation study carried out with the PTC system revealed that as the

water inlet temperature increases, the collector thermal efficiency decreases considerably due to the increase in the value of overall heat loss co-efficient. An optimum value of mass flow rate through the collector could be selected as the flow rate at which the maximum value of thermal efficiency is attained without an excessively high-pressure drop. The mass flow rate indirectly controls the temperature rise across the collector. As the annulus gap between the receiver tube and the glass cover increases, the thermal efficiency decreases due to the increase in receiver tube outside convection heat transfer co-efficient. As the wind velocity increases, the thermal efficiency decreases due to the increase in the glass cover outside heat transfer co-efficient. The performance of the parabolic trough collector system predicted in the present study by the simulation model based on the MATLAB simulation program complies well with its actual performance determined experimentally by other investigators. Therefore, this simulation program can be effectively used to guide the performance of a parabolic trough collector water heating system.

5. REFERENCES

[1] Kalogirou, S. 1996. Parabolic trough collector system for low temperature steam generation-Design and performance characteristics. Applied Energy 55(1): 1-19.

[2] Heinzel, V.; Kungle, H.; and Simon, M. 1995. Simulation of a parabolic trough collector. ISES solar world congress, Harare, Zimbabwe:1-10.

[3] Dudley, V.; Kolb, G.; Sloan, M.; and Kearney, D. 1994. SEGS LS2 solar collector – test results. Report of Sandia National Laboratories: SANDIA94-1884, U.S.A.

[4] Odeh, S.D.; Morrison, G.L.; and Behnia M. 1996. Thermal analysis of parabolic trough solar collector for power generation. In Proceedings of ANZSES 34th Annual conference, Darwin, Australia: 460-467.

[5] Odeh, S.D.; Morrison, G.L.; and Behnia, M. 1998. Modelling of parabolic trough direct steam generation solar collectors. Solar Energy 62: 395-406.

[6] Duffie, J. A. and Beckman, W.A. 1991. Solar Engineering of Thermal Processes- 2nd edition. New York : John Wiley.

[7] Guven, H.M. and Bannerot, R.B. 1985. Derivation of universal error parameters for comprehensicve optical analysis of parabolic troughs. Proceedings of the ASME-ASES Solar Energy Conference. Knoxville, USA: 168-174.

[8] Guven, H.M. and Bannerot, R.B. 1986. Determination of Error Tolerances for the Optical Design of Parabolic Troughs for Developing Countries. Solar Energy 36: 535-550.

[9] Kreith, F. and Kreider, J.F. 1978. Principles of Solar Engineering. New York: McGraw-Hill.

[10] Sukhatme, S.P. 1999. Solar Energy – Principles of thermal collection and storage- Second Edition. New Delhi: Tata McGraw-Hill Publishing Company Limited.

[11] Incropera, F.P. and Dewitt, D.P. 1998. Fundamentals of Heat and Mass Transfer. Fourth edition. New York: John Wiley & Sons.

[12] Kalogirou, S.; Lloyd, S.; Ward, J.; and Eleftheriou, P. 1994. Design and performance characteristics of a parabolic-trough solar-collector system. Applied Energy 47: 341-354.